Regime shift in the destructiveness of tropical cyclones over the western North Pacific

Environmental Research Letters

LETTER

Regime shift in the destructiveness of tropical cyclones over the western North Pacific

Shifei Tu[1,2], Feng Xu[1,2] and Jianjun Xu[1,2]

[1] South China Sea Institute of Marine Meteorology, Guangdong Ocean University, Zhanjiang, People's Republic of China
[2] College of Ocean and Meteorology, Guangdong Ocean University, Zhanjiang, People's Republic of China

E-mail: gdouxufeng@126.com and gmuxujj@163.com

Keywords: tropical cyclones, power dissipation index, regime shift

OPEN ACCESS

RECEIVED
18 June 2018

REVISED
22 August 2018

ACCEPTED FOR PUBLICATION
31 August 2018

PUBLISHED
19 September 2018

Abstract

The characteristics of tropical cyclones (TCs) and their response to climate change is an issue of broad concern. Based on the Power Dissipation Index (PDI) proposed by Emanuel in 2005, the destructiveness of TCs in the typhoon season (July–October) during the period 1979–2016 over the western North Pacific is investigated. Results show that a regime shift in the destructive potential of TCs took place around 1998. The destructive potential of TCs has a considerable increasing trend from 1998 to 2016 (the P2 period), mainly contributed by the average intensity of TCs (51.20% of PDI change). We find that the PDI of TCs is mainly regulated by the El Niño/Southern Oscillation cycle in whole study period, whereas the Pacific Decadal Oscillation pattern shows significant enhancement in P2, which acts as a more important constraint on the typhoon season PDI over the western North Pacific.

1. Introduction

Tropical cyclones (TCs) are one of the most severe and frequent natural disasters on Earth, and their activity poses serious threats to people's lives and property in coastal countries (Peduzzi *et al* 2012, Lin *et al* 2014). With the rapid economic development and growing human population in coastal areas, especially in developing countries, the losses of property stemming from TC activity may worsen (Mendelsohn *et al* 2012). Therefore, it is important to gain an accurate understanding of the potential threats and long-term changes in TC activity (Goldenberg and Gray 2001, Landsea *et al* 2006, Hsu *et al* 2014), especially under a warmer climate (Elsner *et al* 2006, Mendelsohn *et al* 2012, Mei *et al* 2015, Sun *et al* 2017).

In early studies, TC frequency (number of TC geneses) and intensity (usually expressed as the maximum sustained wind speed near the center) were often used to measure the activity of TCs (Emanuel 2000, Landsea *et al* 2006). While this can partly reflect the characteristics of TC activity, there are significant limitations to this approach (Emanuel 2005). To better describe the potential changes in the threats posed by TC activity throughout an event's lifetime, the concept of TC 'destructive potential' has been applied, which combines the contributions of TC intensity, frequency and duration, and thus serves as a better indicator to quantify the potential threat of TCs compared with any one single parameter (Camargo and Sobel 2005).

Emanuel (2005) defined the Power Dissipation Index (PDI) to estimate the TC destructive potential, and found a remarkable upward trend in the PDI over the western North Pacific and North Atlantic basins since the mid-1970s, along with a close relationship between tropical SST changes and this trend. Vecchi *et al* (2008) confirmed that there has been a significant increase in North Atlantic PDI in recent years, and used model predictions to also show that the TC destructive potential will likely increase considerably in the future. However, it has recently been found that the TC destructive potential globally shows a marked decreasing trend from the beginning of the 1990s (Maue 2011). Lin and Chan (2015) explored the features of PDI changes in the typhoon season over the western North Pacific and pointed out a downward PDI trend in the last two decades. Also, high-resolution model predictions like that reported by Zhao and Held (2011) show that the PDI will reduce, probably by 15%, by the end of the 21st century. Thus, there is striking uncertainty in the trends of TC destructive potential regionally and globally.

Building on these previous studies, the purpose of the present study is to re-examine the long-term characteristics of typhoon season PDI in the western North Pacific, and explore whether a new trend in TC destructive potential can be detected in this region against the current background of global warming and, if so, investigate the possible mechanisms involved. The data and methods used in the study are described in section 2. The temporal evolution of the PDI and its related parameters are shown in section 3, the links of the PDI with El Niño/Southern Oscillation (ENSO) and the Pacific Decadal Oscillation (PDO) are investigated in section 4. Several brief discussions are provided in section 5. Finally, some conclusions of this work are shown in section 6.

2. Data and methods

2.1. Regions and datasets

We define the western North Pacific region as (0°–45°N, 110°E–180°), and the main development region (MDR) of TCs as (5°N–30°N, 122°E−180°). We focus on TCs forming over the MDR of the western North Pacific from 1979 to 2016 in the typhoon season (July–October), excluding 'native typhoons' that generated in the South China Sea. The historical TC best-track dataset used in this paper is from the China Meteorological Administration's Tropical Cyclone Center (Ying *et al* 2014), which includes the position, minimum pressure, and maximum two minutes sustained wind speed of TCs every six hours. Due to the higher and regular observation density, this best-track dataset has higher quality over China's land and marginal sea regions.

ENSO and PDO are the strongest signals at interannual and interdecadal scales over the tropical and northern Pacific regions, which have an important role in forming, developing and maturing TCs over the western North Pacific Ocean. Camargo and Sobel (2005) revealed that the TCs generated in El Niño years have longer lifetimes and more intensity, while the TCs formed in La Niña years have short durations and weak intensity. Another study found that PDO can modulate the relationship between ENSO and TCs (Wang and Liu 2016). Thus, to explore the possible links between the PDI and the climatic background, the monthly Nino3.4 index (calculated from ERSST V5 (Huang *et al* 2017)) and the monthly PDO index (Mantua *et al* 1997, obtained from the monthly ERSST V4 data (Huang *et al* 2015)), from 1979–2016, are used. In addition, the monthly ERA-Interim reanalysis dataset, on a 1° grid (Dee *et al* 2011), from ECMWF (European Center for Medium Weather Forecasting), is used to examine the changes in atmospheric conditions such as the vertical wind shear and relative vorticity.

The thermodynamic conditions of the ocean are important in providing sufficient heat for TC activity (Shay and Brewster 2006), and in this context, the depth of the 26 °C isotherm (D26) is used here to represent the upper-ocean heat content. D26 is calculated using the monthly EN4.2.0 oceanic reanalysis dataset from the Hadley Center (Good *et al* 2013).

2.2. PDI and related parameters

The pressure deficit in TC center and the surface maximum sustained wind speed near the TC center are both common indicators of TC intensity. Notwithstanding, it has been pointed out that the central pressure deficit of TCs is more advantageous in explaining historical economic losses induced by TCs than using the maximum sustained wind speed (Chavas *et al* 2017). In contrast to using any single factor (intensity or frequency), however, the TC destructive potential combines the effects of several of the most important parameters and is a good indicator of the threat posed by a TC. We use the PDI proposed by Emanuel (2005), which integrates the contributions of TC number, duration, and intensity to estimate the TC destructive potential. For each typhoon season (July–October), the PDI is calculated as

$$PDI = \sum_{i=1}^{N} \int_0^{\tau_i} {V_{\max}}^3 \, dt,$$

where $V_{\max}$ is the maximum sustained surface wind speed every six hours, τi is the lifetime of each storm, and N is the count of TCs in every typhoon season.

To reduce the interference from uncertainty in the best-track database, Emanuel (2007) proposed a velocity-weighted duration of TC i as

$$D_i = \frac{\int_0^{\tau_i} V_{\max} \, dt}{V_{\mathrm{smax}}}$$

where V_{smax} is the peak sustained wind during the lifetime of the TC, and the average velocity-weighted duration of the annual typhoon season as

$$D = \frac{1}{N} \sum_{i=1}^{N} D_i.$$

To separate the contributions of TC number (N), duration (D) and intensity (I), Emanuel (2007) provided a quantitative way to define the annually accumulated PDI in a typhoon season:

$$\mathrm{PDI} = N \times D \times I.$$

Therefore, the annual average duration-weighted intensity can be defined as

$$I = \frac{\sum_{i=1}^{N} \int_0^{\tau_i} V_{\max}^3 \, dt}{\sum_{i=1}^{N} D_i}.$$

3. Changes in the trends of the PDI and its contributing factors

The typhoon season (July–October) PDI series of TCs in the western North Pacific has fluctuated strongly in

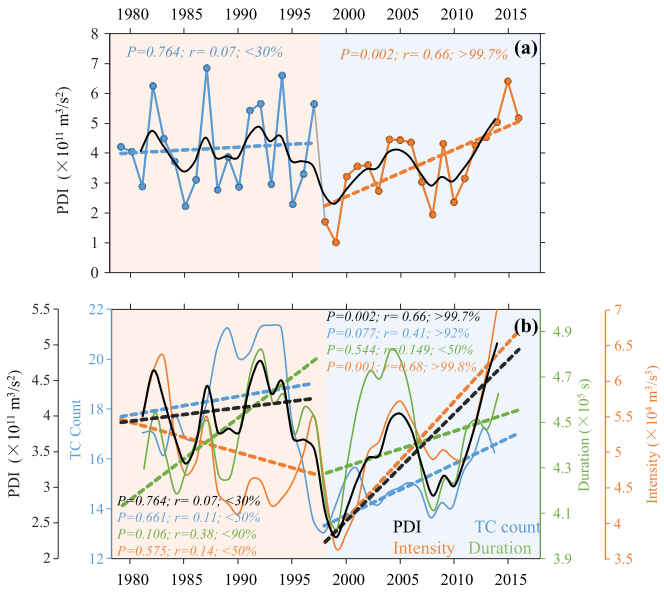

Figure 1. The annual typhoon season PDI and its contributing factors: (a) PDI series over the western North Pacific (0°–45°N, 110°E–180°) during 1979–2016, in which the blue and orange solid lines are for P1 and P2 respectively, the dotted line is the linear trend of the PDI in the two periods, and the black curve is the '1-2-4-2-1' filtered PDI; (b) a '1-2-4-2-1' filtered annual typhoon season time series over the western North Pacific during 1979–2016, in which the blue curve is the TC count (N), the green curve is the average velocity-weighted duration (D), the orange line is the average intensity (I), the black curve is the filtered annual PDI, and the dotted lines are the linear trends of each series in the two periods.

the last few decades (figure 1(a)). There is a significant difference in the PDI between the periods of 1979–1997 and 1998–2016, and so we define the former as P1 and the latter as P2. The linear trend of the PDI during P1 is one of a slight increase. Then, the PDI declines rapidly during 1997–1998, before showing considerable growth during the following stage (i.e., P2). Thus, the potential damage of TCs shows a significant regime shift around 1998, despite some technical and factitious changes in this track dataset (Ying *et al* 2014), but the regime change around 1998 was also exhibited in both JMA (Japan Meteorological Agency) and JTWC (Joint Typhoon Warning Center) best-track datasets (figure not shown). The PDI in the last five years of the study period (2012–2016) increases by approximately 96.50% compared with 1998–2003, with an average growth rate of $1.48 \times 10^{10}\ \mathrm{m^3\ s^{-2}}$ per year. This growth PDI is in opposition to the negative trend found by Lin and Chan (2015) because this mutation of PDI around 1998 was not noted in their work due to the shorter research period.

As mentioned in section 2, above, and in Emanuel (2007), the PDI is determined by the TC frequency (number of typhoon season TC geneses: N), intensity (the cube of the maximum sustained wind speed: I), and the duration (defined as a velocity-weighted duration: D). We examine the changes in these three PDI factors. In order to better show the low-frequency characteristics of the time series, we defined a '1-2-4-2-1' filter as:

$$\overline{x_i} = \frac{1}{10}(x_{i-2} + 2x_{i-1} + 4x_i + 2x_{i+1} + x_{i+2})$$

where $\overline{x_i}$ is the filtered result, figure 1(b) shows the '1-2-4-2-1' filtered time series curve of N (in blue), average D (in green) and average I (in orange) in the typhoon season over the western North Pacific. It shows that there are some differences between the two periods: N increases remarkably in P1 to begin with, but a drastic decreasing trend appears in the latter part of P1 in around 1995—a regime shift that has been highlighted in several previous studies (Matsuura *et al* 2003, Liu and Chan 2013, Hsu *et al* 2014). In the early part of P2, the trend remains one of lower magnitude until 2013, after which it begins to increase again during 2013–2016.

The average velocity-weighted D (figure 1(b)) has no significant change statistically in both periods. The average I time series shows a remarkably opposite trend between the two periods, with a significant reduction in P1 and a considerable increase in P2. The trend of the average I in P2 is basically consistent with the PDI (figure 1(b)).

Furthermore, we calculate the contribution rates of the three factors to the PDI in the two periods using linear regression analysis. The results indicate that the change in the PDI during P1 is mainly contributed by the average D, which can explain 51.84% of the PDI change (table 1), but this contribution decreases to 28.80% in P2. The contribution of the average I to the PDI becomes gradually dominant in P2, explaining up to 51.20% of the PDI change. This indicates that the changes in the destructive potential of TCs in P2 are mostly contributed by the average I.

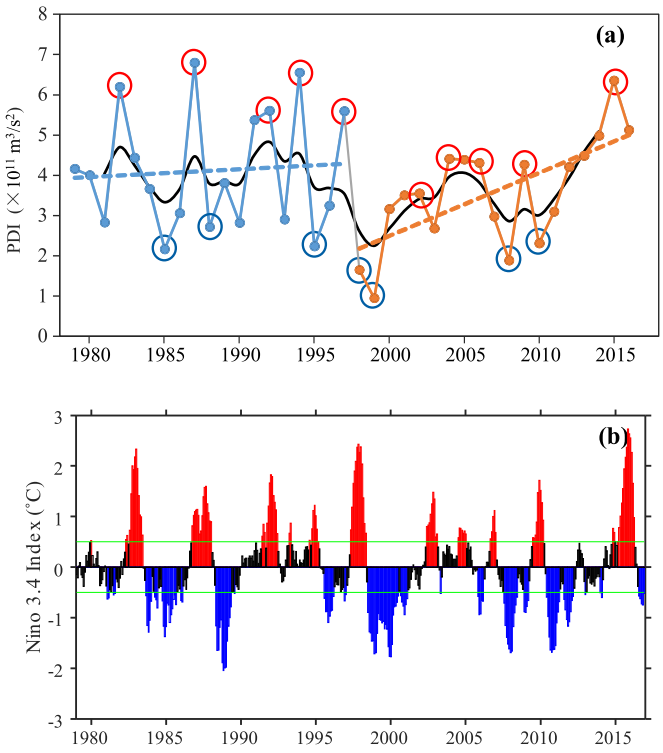

Figure 2. Annual PDI time series (a) and monthly (January–December) Niño 3.4 index (b). The red and blue circles in (a) represent typical El Niño and La Niña years respectively, and the red and blue bars in (b) indicate that Niño 3.4 is greater than 0.5 °C and less than −0.5 °C, with black bars for Niño 3.4 index values between −0.5 °C and 0.5 °C.

Table 1. Contribution rates to the PDI. 'Correl.' is the correlation coefficients between the three contributing factors and the PDI, and '%' represents the contribution rates of the different factors in the two periods. An asterisk indicates statistical significance at the 95% confidence level.

	TC count (N)		Duration (D)		Intensity (I)	
Contribute rate	Correl.	%	Correl.	%	Correl.	%
P1	0.18	2.91	0.76*	51.84*	0.71*	45.25*
P2	0.55*	20.00*	0.66*	28.80*	0.88*	51.20*

Table 2. Correlations among different series during the two periods. An asterisk indicates statistical significance at the 95% confidence level.

Correlation		PDI	TC count (N)	Duration (D)	Intensity (I)	D26	PDO	Nino 3.4
P1 (1979–1997)	PDI	1						
	TC count (N)	0.18	1					
	Duration (D)	0.76*	−0.06	1				
	Intensity (I)	0.71*	−0.46*	0.49*	1			
	D26	−0.46*	0.28	−0.73*	−0.39	1		
	PDO	−0.14	−0.57*	0.13	0.55*	−0.30	1	
	Niño3.4	0.72*	−0.22	0.77*	0.64*	−0.80*	0.40	1
P2 (1998–2016)	PDI	1						
	TC count (N)	0.55*	1					
	Duration (D)	0.66*	0.05	1				
	Intensity (I)	0.88*	0.21	0.53*	1			
	D26	−0.77*	−0.10	−0.77*	−0.72*	1		
	PDO	0.61*	0.01	0.43*	0.71*	−0.82*	1	
	Nino3.4	0.71*	0.11	0.80*	0.60*	−0.83*	0.67*	1

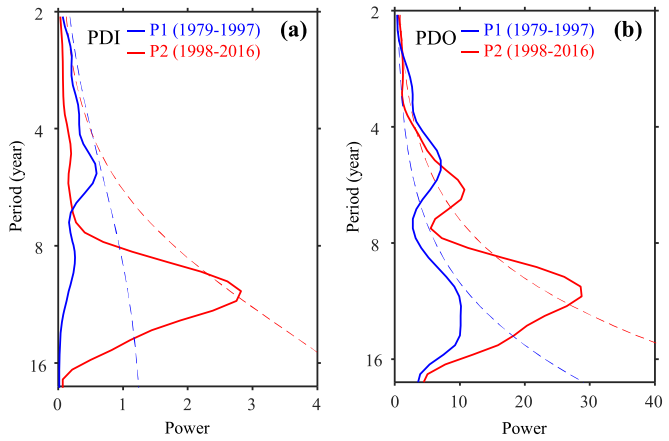

Figure 3. Comparison of the power spectra for the PDI and PDO in the two periods: (a) power spectrum of the 21-term running average of monthly PDI (this PDI series is divided by 10^{11}), in which P1 is in blue and P2 in red; (b) as in (a) but for the monthly PDO index, in which the dashed line is the 95% confidence interval against red noise in P1 and P2. The result shows that the periodicities of the PDO and PDI on the quasi-decadal scale enhance obviously during 1998–2016.

4. Impacts from ENSO and the PDO

It is important to recognize the factors influencing changes in the TC destructive potential in the typhoon season on an annual basis over the western North Pacific. Based on the results presented in figure 1(a), which shows that the PDI has strong interannual oscillations during P1 and P2, we begin by exploring the possible effects of ENSO on the PDI. The correlation (table 2) between the PDI and the Niño 3.4 index indicates significant regulation of the PDI by ENSO during P1 and P2, and the fluctuation in the PDI corresponds well with El Niño and La Niña events (figure 2). This shows that ENSO has a remarkable impact on the interannual-scale destructive potential of TCs in the western North Pacific, which is consistent with another work (Camargo and Sobel 2005).

Table 2 shows the relationship of ENSO and PDI during the P1 and P2 periods; it is contended that there is a commensurate correlation between ENSO and PDI both in P1 and P2 periods. However, the impacts from ENSO on the PDI related parameters have some differences: D has the strongest relation with ENSO which is increased in the P2 period, and I is also modulated by ENSO. Meanwhile, there was no significant relation between ENSO and the TC count during 1979–2016.

Alongside the interannual variation, the destructive potential in the western North Pacific shows a distinct interdecadal shift, and so we also examine the effects of the PDO. The correlation between the average PDO index in the typhoon season and the PDI is calculated, and the results (table 2) indicate no significant correlation between the PDO and PDI during P1, but a much closer relationship in P2. Thus, the power of the PDO's control over the destructive potential of TCs in the western North Pacific clearly enhances, which is mainly reflected in the D and I. The reason is that the PDO's pattern notably enhances during P2 and the power spectrum results demonstrate that the periodicities of the PDO and PDI on the quasi-decadal scale obviously enhance during P2 (figure 3). Thus, the relationship between the PDO and PDI is much closer in that period.

5. Discussion

The change in intensity is closely related to the thermal conditions of the upper ocean (Goni *et al* 2009, Mei *et al* 2015). We defined a 26 °C isotherm depth index (D26) as the mean depth of the 26 °C isotherm over the MDR; this is used to measure the upper-ocean heat content. The results (table 2) show that the correlation coefficient between the D26 and the PDI is strong during P2. This indicates that the thermal conditions of the upper ocean are more closely related to the PDI during P2 than during P1.

But why does the destructive potential of TCs weaken in the western North Pacific in conjunction with an increasing D26? Recent evidence has revealed that the temperature in the deep ocean increases during the negative phase of the PDO (Meehl *et al* 2011, England *et al* 2014). Our results also indicate a huge increase in the subsurface heat content over the western North Pacific (figure 4). As a result, heat transported westward from the central and eastern Pacific has been divided into two parts; the more heat is stored in the deep ocean, the less energy is provided for TCs.

Lin and Chan (2015) emphasized that the decrease in the PDI that they detected was mainly due to the contributions of TC frequency and duration. Exploring the causes of PDI reduction from the perspective of atmospheric dynamics, it was found that atmospheric conditions (the subtropical high, vertical wind shear, relative vorticity at 850 hPa, and so on) provide stronger 'worsened' conditions for TC activity than the 'better' oceanic thermal conditions under the global

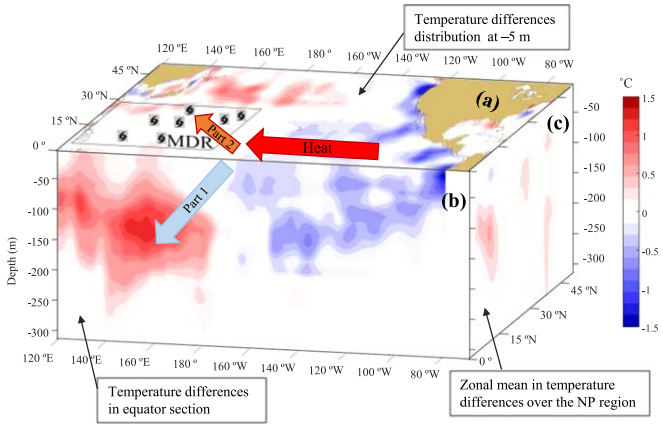

Figure 4. The upper-ocean thermodynamic structure differences in the North Pacific between the two periods, wherein the temperature differences are calculated as P2 minus P1, and the upper-ocean temperature data are from the monthly EN4.2.0 oceanic reanalysis dataset provided by the Hadley Center: (a) longitude–latitude section of the distribution of temperature differences at −5 m; (b) longitude–depth section of the differences in temperature at the equator; (c) latitude–depth section of the zonal mean temperature differences over the North Pacific region. The heat transported from the central and eastern equatorial Pacific has been divided into two parts; the larger part (i.e., Part 1) is stored in the deep ocean and the smaller part (i.e., Part 2) is provided for the TC activity in P2.

Table 3. Correlations among different parameters during these two periods. The vertical wind shear (the differences of wind field at 200 hPa and 850 hPa) is the regional mean of the MDR, and the relative vorticity at 850 hPa is also the average result of the MDR. An asterisk indicates statistical significance at the 95% confidence level.

	Correlation	PDI	Nino 3.4	PDO
P1 (1979–1997)	Genesis Lon.	0.75*	0.73*	0.19
	Genesis Lat.	−0.36	−0.54*	−0.65*
	Wind Shear	−0.09	−0.27	−0.11
	Relative Vorticity	0.67*	0.75*	−0.11
P2 (1998–2016)	Genesis Lon.	0.67*	0.74*	0.61*
	Genesis Lat.	−0.64*	−0.73*	−0.70*
	Wind Shear	−0.62*	−0.44*	−0.57*
	Relative Vorticity	0.71*	0.87*	−0.50*

warming scenario. Our results, however, show the PDI changes to be mainly due to differences in the distribution of heat (i.e., stored in the deep ocean or provided for TC activity) transported from the central and eastern tropical Pacific (figure 4). This indicates that there are significant differences in the allocation of dynamic and thermal factors affecting TC activities in the western North Pacific during the different research periods.

It is undeniable that vertical wind shear and the relative vorticity of the lower atmosphere are two important factors affecting TC activity. Similarly, we found that the relationship between vertical wind shear and the PDI has a huge discrepancy in the two periods; the correlation is obviously increased in the P2 period (i.e. −0.09 in P1 and −0.62 in P2 period, table 3), and it may be controlled by the strengthened PDO in this period (increase from −0.11 to −0.57, table 3). It is shown that the regime shift of the PDI is not only caused by the change in the upper-ocean thermal conditions but also influenced by the atmospheric vertical shear. Meanwhile, the relative vorticity and PDI have a positive correlation in both periods.

In addition, we find that the PDI change is mainly affected by the ENSO cycle. When the equatorial easterly winds strengthen at the onset of a La Niña event, a large amount of warm water in the central and eastern Pacific region is transported westward, resulting in increased heat content in the warm pool region, and accompanied by a generally westward TCs genesis location (table 3), which leads to an obvious decrease in the PDI. The situation is the opposite in El Niño years: positive SST anomalies in the central Pacific region are conducive to atmospheric convection. Disturbances (or typhoon embryos) form easily and, as a result, the average intensity and PDI are elevated in El Niño years.

ENSO, reflected the interannual-scale oscillations, mainly occurs in the tropical Pacific region, so it has a more direct impact on TC activity via the Walker circulation (Wang and Liu 2016) and the upper-ocean heat transport in the tropical Pacific region (figure 4). Therefore, the TC intensity and locations in the western North Pacific are determined by the strength of ENSO. In contrast, the interdecadal scale influence on TCs primarily comes from PDO. Its constraint ability for TCs is mainly through the teleconnection way via forcing the atmospheric dynamical conditions; partially, the vertical wind shear (table 3). This power is greatly affected by the PDO intensity and phases, and we found that the strength and phases of PDO are different in P1 and P2, thus the influences on the TCs destructive potential have changed greatly during the P1 and P2 periods (figure 3).

Several studies (Mantua and Hare 2002, Macdonald and Case 2005, Diaz *et al* 2010) contend that ENSO and PDO both have a variable frequency, but how will the impacts of ENSO and PDO on TCs activity change? Our findings, in table 2, reveal that the relation of TCs activity and PDO will change obviously during P1 and P2 (figure 3), while there is no significant variation in the relationship of ENSO and TCs during these two periods.

The active areas of TCs are not always stationary. Recent studies have pointed out that there is a significant poleward migration in the global TCs (Kossin *et al* 2014, Tamarin-Brodsky and Kaspi 2017), which may be related to Hadley cell expansion (Sharmila and Walsh 2018). Hadley cell change associated with the expansion of the tropical belt, which can lead to the gradual poleward shift of TC-favorable climate conditions. Additionally, the poleward location of the anomaly of the Hadley cell upward branch is more clear in the western North Pacific region (Sharmila and Walsh 2018). Combined with the maximum TC count over the world, the potential damage of TC-induced may increase in the higher latitude of the western North Pacific region.

6. Conclusions

This paper analyzes the long-term evolution of the PDI in the typhoon season over the western North Pacific. We find that a regime shift in the PDI took place around 1998. The PDI indicates a negligible increase in destructiveness during the P1 period (1979–1997), but then a remarkable increase during the P2 period (1998–2016). Here, the results show that D and I are found to play a critical role in the evolution of the PDI during P1, with contribution rates of 51.84% and 45.25% respectively. During P2, however, the contribution of D reduces to 28.80%, and that of I enhances to 51.20%. The role of N is relatively small in both periods.

The 1998 regime shift of the destructive potential of TCs over the western North Pacific is restricted by the upper-ocean thermal conditions; in addition the vertical shear of the atmosphere also changes greatly in the P2 period, which also has a remarkable role in this changing PDI. Meanwhile, the relationship between relative vorticity and PDI change during the P1 and P2 periods are negligible.

ENSO and PDO both have strong influences on the TCs over the western North Pacific. The impacts from ENSO is mainly reflected in the interannual scale, and the restraint to the destructive potential of TCs remains basically unchanged in the two periods. In El Niño year, PDI is relatively larger than the PDI in La Niña year, while PDO mainly regulates the interdecadal scale oscillations of PDI, and this link is related to the strength and phases change of PDO. PDO modulates the destructive potential of TCs via atmospheric conditions such the vertical wind shear.

This increasing trend in the PDI during P2 is due to the impacts from the super La Niña that erupted in 1998–2001 and the strong El Niño in 2014–2016, as well as the decadal variation in the PDI forced by a quasi-decadal oscillation of the PDO during this period.

Our findings may have important implications for an accurate understanding of the long-term evolution of TC destructive potential over the western North Pacific, the effects of ENSO and PDO on TCs' potential damage, and the role of atmospheric and oceanic conditions on TC activity change.

Acknowledgments

This research was supported by the National Key R&D Program of China through grants 2018YFA0605604 and 2017YFC1501802, the Strategic Priority Research Program of Chinese Academy of Sciences through grant XDA20060503 and the State Key Laboratory of Natural Disasters. The authors declare no competing financial interests. We thank the CMA (http://tcdata.typhoon.org.cn/), NOAA (https://www.esrl.noaa.gov/psd/data/gridded/), ECMWF (http://apps.ecmwf.int/datasets/data/interim-full-moda/levtype=pl/) and Hadley Center (http://hadobs.metoffice.com/index.html) for the availability of the data used in this work.

ORCID iDs

Shifei Tu https://orcid.org/0000-0003-3720-6259

References

Camargo S J and Sobel A H 2005 Western North Pacific tropical cyclone intensity and ENSO *J. Clim.* **18** 2996–3006

Chavas D R, Reed K A and Knaff J A 2017 Physical understanding of the tropical cyclone wind-pressure relationship *Nat. Commun.* **8** 1360

Dee D P *et al* 2011 The EAR-Interim reanalysis: configuration and performance of the data assimilation system *Q. J. R. Meteorol. Soc.* **137** 553–97

Diaz H F, Hoerling M P and Eischeid J K 2010 ENSO variability, teleconnections and climate change *Int. J. Climatol.* **21** 1845–62

Elsner J B, Tsonis A A and Jagger T H 2006 High-frequency variability in hurricane power dissipation and its relationship to global temperature *Bull. Am. Meteorol. Soc.* **87** 763–8

Emanuel K 2000 A statistical analysis of tropical cyclone intensity *Mon. Weather Rev.* **128** 1139–52

Emanuel K 2005 Increasing destructiveness of tropical cyclones over the past 30 years *Nature* **436** 686–8

Emanuel K 2007 Environmental factors affecting tropical cyclone power dissipation *J. Clim.* **20** 5497–509

England M H *et al* 2014 Recent intensification of wind-driven circulation in the Pacific and the ongoing warming hiatus *Nat. Clim. Change* **4** 222–7

Goldenberg S B and Gray W M 2001 The recent increase in Atlantic hurricane activity: causes and implications *Science* **293** 474–9

Goni G, Demaria M, Knaff J and Sampson C 2009 Applications of satellite-derived ocean measurements to tropical cyclone intensity forecasting *Oceanography* **22** 190–7
Good S A, Martin M J and Rayner N A 2013 EN4: Quality controlled ocean temperature and salinity profiles and monthly objective analyses with uncertainty estimates *J. Geophys. Res. Oceans* **118** 6704–16
Hsu P C, Chu P S, Murakami H and Zhao X 2014 An abrupt decrease in the late-season typhoon activity over the western North Pacific* *J. Clim.* **27** 4296–312
Huang B *et al* 2015 Further exploring and quantifying uncertainties for extended reconstructed sea surface temperature (ERSST) version 4 (v4) *J. Clim.* **29** 3119–42
Huang B *et al* 2017 Extended reconstructed sea surface temperature version 5 (ERSSTv5), upgrades, validations, and intercomparisons *J. Clim.* **30** 8179–205
Kossin J P, Emanuel K A and Vecchi G A 2014 The poleward migration of the location of tropical cyclone maximum intensity *Nature* **509** 349–52
Landsea C W, Harper B A, Hoarau K and Knaff J A 2006 Climate change. can we detect trends in extreme tropical cyclones? *Science* **313** 452–4
Lin I I, Pun I F and Lien C C 2014 'category-6' super typhoon Haiyan in global warming hiatus: contribution from subsurface ocean warming *Geophys. Res. Lett.* **41** 8547–53
Lin I I and Chan J C L 2015 Recent decrease in typhoon destructive potential and global warming implications *Nat. Commun.* **6** 7182
Liu K S and Chan J C L 2013 Inactive period of western North Pacific tropical cyclone activity in 1998–2011 *J. Clim.* **26** 2614–30
Macdonald G M and Case R A 2005 Variations in the Pacific decadal oscillation over the past millennium *Geophys. Res. Lett.* **32** L08703
Mantua N J, Hare S R, Zhang Y, J. Wallace M and Francis R C 1997 A Pacific interdecadal climate oscillation with impacts on salmon production *Bull. Am. Meteorol. Soc.* **78** 1069–79
Mantua N J and Hare S R 2002 The Pacific decadal oscillation *J. Oceanog.* **58** 35–44
Matsuura T, Yumoto M and Iizuka S 2003 A mechanism of interdecadal variability of tropical cyclone activity over the western North Pacific *Clim. Dyn.* **21** 105–17
Maue R N 2011 Recent historically low global tropical cyclone activity *Geophys. Res. Lett.* **38** 14803
Meehl G A, Arblaster J M, Fasullo J, Hu T A and Trenberth K E 2011 Model-based evidence of deep-ocean heat uptake during surface-temperature hiatus periods *Nat. Clim. Change* **1** 360–4
Mei W, Xie S P, Primeau F, James C M and Claudia P 2015 Northwestern Pacific typhoon intensity controlled by changes in ocean temperatures *Sci. Adv.* **1** e1500014–1500014
Mendelsohn R, Emanuel K, Chonabayashi S and Bakkensen L 2012 The impact of climate change on global tropical cyclone damage *Nat. Clim. Change* **2** 205–9
Peduzzi P *et al* 2012 Global trends in tropical cyclone risk *Nat. Clim. Change* **2** 289–94
Sharmila S and Walsh K J E 2018 Recent poleward shift of tropical cyclone formation linked to Hadley cell expansion *Nat. Clim. Change* **8** 730–6
Shay L K and Brewster J K 2006 Oceanic heat content variability in the eastern Pacific ocean for hurricane intensity forecasting *Mon. Weather Rev.* **138** 2110–31
Sun Y *et al* 2017 Impact of ocean warming on tropical cyclone size and its destructiveness *Sci. Rep.* **7** 8154
Tamarin-Brodsky T and Kaspi Y 2017 Enhanced poleward propagation of storms under climate change *Nat. Geosci.* **10** 1–6
Vecchi G A, Swanson K L and Soden B J 2008 Whither hurricane activity? *Science* **322** 687–9
Wang X and Liu H 2016 PDO modulation of ENSO effect on tropical cyclone rapid intensification in the western North Pacific *Clim. Dynam.* **46** 15–28
Ying M, Zhang W and Yu H 2014 An overview of the China meteorological administration tropical cyclone database *J. Atmos. Oceanic Tech.* **31** 287–301
Zhao M and Held I M 2011 TC-permitting GCM simulations of hurricane frequency response to sea surface temperature anomalies projected for the late-twenty-first century *J. Clim.* **25** 2995–3009